

We are IntechOpen, the world's leading publisher of Open Access books Built by scientists, for scientists

6,900

Open access books available

185,000

International authors and editors

200M

Downloads

Our authors are among the

154

Countries delivered to

TOP 1%

most cited scientists

12.2%

Contributors from top 500 universities



WEB OF SCIENCE™

Selection of our books indexed in the Book Citation Index
in Web of Science™ Core Collection (BKCI)

Interested in publishing with us?
Contact book.department@intechopen.com

Numbers displayed above are based on latest data collected.
For more information visit www.intechopen.com



A Simple Approach to the Study of the Ageing Behaviour of Laser Beam and Friction Stir Welds between Similar and Dissimilar Alloys

Claudio Badini¹, Claudia Milena Vega Bolivar¹, Andrea Antonini¹, Sara Biamino¹, Paolo Fino¹, Diego Giovanni Manfredi², Elisa Paola Ambrosio², Francesco Acerra³, Giuseppe Campanile³ and Matteo Pavese¹

¹*Politecnico di Torino, Dipartimento di Scienza dei Materiali e Ingegneria Chimica*

²*IIT, Italian Institute of Technology, Center for Space Human Robotics @ PoliTO*

³*Alenia Aeronautica S.p.A., Materiali e Processi, Italy*

1. Introduction

In recent years, lightweight structures have become more and more important for the transportation industry, since they allow reduction of fuel consumption and thus atmospheric pollution. The most common light metal is aluminium, that has a density close to 2.7 g/cm³ coupled with interesting mechanical properties. Until 50 years ago, however, aluminium alloys were considered not weldable, due to the formation of aluminium oxide. Nowadays, the welding of aluminium is a well-known and much studied subject, since welds are often the weak point of a structure. Indeed, aluminium alloys are mainly reinforced by controlled ageing or plastic deformation, so that welds represent an area of the structure where the standard approach for improving mechanical properties is not applicable. On the other side, mechanical fastening or riveting brings to serious problems during application, so that a significant effort has been done to develop low cost and high efficiency joining techniques.

The most used welding techniques are based on the localised melting of the alloys to be joined. The most common are MIG (metal inert gas welding), an arc welding under inert atmosphere with a metal fusible electrode, generally supplied with continuous current at inversed polarity, and TIG (tungsten inert gas welding), that is an arc welding under inert atmosphere with a tungsten electrode, often supplied with alternate current. These techniques avoid the formation of dangerous inclusions, by favouring the oxide removal and protecting the molten metal by inert gas. Oxyfuel and electrical resistance welding are also used, while the most recent techniques use plasma, an electron beam or a laser to induce melting and welding. Recently, friction techniques have gained much support, since they avoid melting of the involved alloys.

General considerations about welding of aluminium alloys must take into account several features of this kind of process. First, aluminium is a good heat conductor, so that localized melting is difficult. Wide deformations and microstructure modifications are observed, since temperature is high even far from the weld. Second, aluminium is oxidised very easily, with

alumina formation. Inclusions in the weld are often obtained, or the formation of oxide films or veils can be observed. Third, gaseous inclusions can be formed during welding, due for instance to the hydrogen solubility in aluminium. With high welding rates (MIG), gases have not the time to go out from the surface of the metal, so that porosity can develop. Hydrogen can be present either in the alloy or in the filler, but alloys are now carefully treated to lower the hydrogen concentration. However surface abrasions can make easier for impurities to enter the metal during working and storage, or hydrogen-rich products can be present on the surface, so that an accurate cleaning of both alloy and filler must be performed before welding. Humidity can be also a clue, since the presence of hydrated metal oxides on the surface can bring to the dissolution of hydrogen during welding. Similarly, the protective gas must not contain impurities, and have a very low dew point. As it happens for many metals, post-weld hot cracking can also occur due to grain growth.

A further difficulty in the welding technology is the requirement, typical for aerospace industry, of joining dissimilar alloys. In aircraft fuselages, for instance, stringers attached to the skin are considered as an important step toward the elimination of mechanically fastened stiffeners; however, this implies the ability of welding together two alloys for example of the 2000 and 7000 series.

In this chapter, two of the most interesting techniques for joining dissimilar alloys are considered: laser beam welding (LBW) and friction stir welding (FSW).

LBW is a melting technique, that uses a source with a high power density (a solid-state or gas laser, rarely a fibre laser) to locally melt a filler wire positioned between the two alloys to be welded. The method is recognized as a rather mature joining technology (Zhao et al. 1999), even if it faces the common drawbacks linked to the fusion welding approach: porosity, hot cracking, low mechanical strength of fusion (FZ) and heat affected zones (HAZ).

To overcome the weaknesses of this technique some care must be taken: a significant attention to the process and to the use of protective atmosphere can reduce hydrogen cracking, occurring grace to the decrease of hydrogen solubility in the fusion zone (FZ). Use of special alloys can reduce solidification cracking (Norman et al. 2003) and the choice of the filler wire can be strategic (Cicala et al., 2005; Braun, 2006). For instance, an Al-12Si alloy can be used with good results, since it avoids the formation of the Mg_2Si phase, that is thought to enhance the solidification cracking susceptibility (Cicala et al., 2005). The control on the process parameter is also extremely important, in particular with dissimilar alloys, and pre- and post-weld treatments can be essential to optimize the weld properties (Braun, 2006; Badini et al., 2009).

Friction stir welding (FSW) was invented at The Welding Institute (UK) in 1991 and is becoming an attractive alternative to conventional bonding techniques for high-performance structural applications in both aerospace and automotive industry. FSW is used mainly with aluminium alloys, even if copper alloys, titanium, steel and magnesium alloys have been welded by this technique. (Mishra & Ma, 2005; Nandan et al., 2008)

The method is based on the production by friction of a thermo-mechanically plasticized zone in the materials to be welded. A rotating tool is put on the contact line between two adjacent metal sheets, and mechanical pressure is applied while the tool is moving along the line of the joint. The tool consists basically in a shoulder and a pin, that from simple cylinders evolved in the last years into more complex shapes (Mishra & Ma, 2005; Thomas et al., 2003; Hirasawa et al., 2010). The tool rotation and applied pressure brings to the movement of matter in the pin zone, with a very complex behaviour. As a result of heat development, plastic deformation and matter movement, a joint is produced with a solid

state process, without the formation of a liquid phase as in more conventional welding techniques. The main parameters of FSW are the tool rotation rate, and the tool transverse speed. The direction of rotation is important for dissimilar alloys welding, where the two sides of the weld, the retreating (tool rotation goes against tool movement along the line of the joint) and the advancing one, correspond to different materials.

FSW shows some advantages over traditional welding techniques involving material melting. First, no added metal is needed, so that many problems related to composition compatibility are overcome, suggesting an easier welding of dissimilar alloys. Second, the total energy consumption of the process is much lower than conventional methods, and there is no need to work with protective gas. Finally, the microstructure of the welds is often very good, with limited porosity, no hot cracking and low residual stresses, that brings to very interesting properties of the joints. However, this method needs expensive equipments and it is easily applicable only for joining plates or components with quite simple geometry, e.g. flat, L and T (Mishra & Ma, 2005).

During FSW, metal flows around the tool, following its rotation, and high temperatures develop. The microstructure of the joint is thus determined by these two phenomena. Metal flow is rather complex and yet poorly understood, and yet is the key parameter to optimize the tool composition and geometry, and FSW parameters (Reynolds, 2000; Reynolds, 2008; Yang et al., 2010). Basically, it was observed that: advancing and retreating sides behave very differently; the movement occurs both on the plane of the weld but also vertically; the alloys are not always mixed with a regular flow, but random distribution of the two alloys can occur, in particular on the top surface; often, however, alternating shapes (bands, lamellae, onion rings,...) are observed of the two metals, depending in any case on the geometry of the tool. Some authors suggest that FSW can be partially compared to an extrusion process (Krishnan, 2002a; Buffa et al., 2006).

The temperature reached during FSW is rather high, due to the intense plastic deformation occurring around the rotating tool and to the friction between the tool and the welded material (Mendez et al., 2010; Hamilton et al., 2008; Sato et al., 1999; Murr et al., 1998). It is clear that the microstructure of the weld is heavily influenced by these phenomena, in particular concerning grain size, grain boundaries, type, size and shape of precipitates. The microstructure will then influence the mechanical behaviour of the weld. In the central zone of the weld, temperature can reach almost 500 °C, so that dissolution of precipitates can occur. This depends however on the specific alloy, since it is reported both dissolution (Sato et al., 1999) and permanence (Murr et al., 1998) of precipitates in the central part of the weld. In any case, it is rather accepted that the maximum temperature is observed at the centre of the weld, and that there is an isothermal zone positioned under the pin (Mishra & Ma, 2005). As the distance from the weld centre grows, the temperature decreases. It has been suggested (Sato et al., 2002) that the temperature grows with the tool rotation rate, while the heating rate depends on the transverse speed, and that on the advancing side the temperature is slightly higher than on the retreating side.

The combined effect of temperature and tool movement produces a very characteristic microstructure of FSW welds. In the stirred zone, where severe plastic deformation occurs, recrystallization and development of texture can be observed, together with precipitates dissolution and/or coarsening (Kwon et al., 2003; Charit & Mishra, 2003; Sauvage et al., 2008). Three main zones, shown in Figure 1, can be discerned: the nugget, corresponding to the stirred zone; the thermo-mechanically affected zone (TMAZ); the heat-affected zone (HAZ).



Fig. 1. Typical image of a weld obtained by FSW.

The nugget consists generally in a recrystallized zone with small grain size, with a shape that depends on the alloy type, the tool geometry and the processing parameters. Generally the nugget has either the shape of an ellipse or that of a wide glacial valley (Mahoney et al., 1998; Sato et al., 1999, Mishra & Ma, 2005). The microstructure is often characterised by fine equiaxed grains of a few microns size, even if sub-micrometric grains can be obtained by using special tools or by cooling the plate immediately after the weld (Kwon et al., 2003; Su et al., 2003; Benavides et al., 1999). Regarding precipitates in the nugget zone, they can either be dissolved or coarsen, depending on the temperature and the alloy composition.

The TMAZ is a sort of transition zone between the nugget and the base metal (Mahoney et al., 1998). In this case, deformation occurs but not recrystallization, so that elongated grains are observed, with a pattern that follows the metal flow induced by the tool movement. High temperature is also present in this zone, so that precipitates dissolution can be sometimes observed (Sato et al., 1999).

The HAZ is simply a zone of the base metal that suffers high temperature due to the heat generated by plastic deformation in the nugget and TMAZ zones (Sato et al., 1998). The very significant increase of temperature in the HAZ can cause precipitation and/or precipitates coarsening, with a negative effect on the mechanical properties (Jata et al., 2000).

During FSW, due to the complex deformation pattern and to the high temperature gradients, residual stresses develop in the weld. The study of residual stresses suggests that their magnitude is much lower than in the case of traditional fusion welding (Peel et al., 2003; Fratini et al., 2009; Hatamleh et al., 2008). The stresses often presents an M shape, with the maximum stress close to the HAZ. The reason for this behaviour can be found in the fact that recrystallization reduces the extent of residual stresses, that is higher at the interface between the mechanical stressed zone and the heat-affected zone. This can be also due to the strong mechanical restraints needed for FSW (Mishra & Ma, 2005). No very significant differences were observed between the advancing and the retreating side of the weld.

Concerning the mechanical properties of the weld, it is important to consider both precipitation-hardened and solid-solution-hardened aluminium alloys, since hardness and other properties depends heavily on the alloy type. In particular, concerning precipitation-hardened alloys, it is generally observed a region in the centre of the weld where hardness is lower than in the base alloys (Sato et al., 1999). This behaviour has been generally ascribed to the coarsening and/or dissolution of the precipitates due to the high temperatures developed during FSW. Instead, in the case of solid-solution-hardened aluminium alloys, no reduction in hardness is generally observed in the weld (Svensson et al., 2000).

Tensile strength of the welds obtained by FSW has been much studied in the past (Mishra & Ma 2005). This welding method brings to rather high mechanical resistance, if compared with standard fusion welding techniques. In particular it seems that in the nugget the reduction of mechanical properties is not very high, while the weak point of the weld is the interface between TMAZ and HAZ (Mahoney et al., 1998). There, on the retreating side, failure generally occurs. Elongation at fracture generally decrease, because the strain is not anymore uniform along the sample, but is concentrated in the low-resistance zone. A post-

weld aging treatment is needed on the precipitation-hardened alloys, in order to improve yield and ultimate strength, even if complete recovery of the elongation of the base alloys is not generally attained (Sato & Kokawa, 2001; Krishnan, 2002b; Sullivan & Robson, 2008; Malarvizhi & Balasubramanian, 2010).

Regarding fatigue resistance, FSW brings to a reduction of the fatigue strength at 10^7 cycles (Di et al., 2006; Jata et al., 2000; Uematsu, 2009), but this behaviour is believed to be strongly correlated with the bad surface finishing of FSW welds. A surface treatment with removal of a portion of the surface improves the fatigue properties close to those of the base metal. In any case it seems that friction stir welds behave better than those obtained by fusion welding methods.

Fracture toughness of FSW welds has been measured both as significantly higher than that of the base metal (Kroninger & Reynolds, 2002; Mishra & Ma, 2005) and as lower than the base metal (Derry & Robson, 2008). In the first case, this happens both in nugget zone and in HAZ/TMAZ region, even if in this latter case the values are lower than in the nugget. This behaviour is probably due to the presence of a finer microstructure, and finer precipitates, even if other mechanisms can be considered, like the presence of particle free zones (PFZ), the bonding strength between alloy and precipitates, the presence of low energy grain boundaries. In the case of lower toughness than base metal, the precipitate coarsening is the main cause of this phenomenon.

As already pointed out, FSW is a very interesting method for the welding of dissimilar alloys and metals (Mishra & Ma, 2005; Murr, 2010; Dubourg et al., 2010; Kwon et al., 2008; Uzun et al., 2005; Lee et al., 2003). In this case, the study of the welds is more complex, and literature is not univocal about the best approach to the welding treatment. For instance, it is reported that the low-strength alloy must be placed on the retreating side, but also on the advancing, in order to improve the weld strength. The microstructure in the nugget seems to be determined by the retreating side material, and joining two precipitate-hardened alloys brings generally to the failure of the weld in the HAZ, where over-aged precipitates are present. This does not seem to reduce substantially fatigue properties, though.

In any case, the papers already published all suggests that FSW is a very promising technique for joining dissimilar alloys with defect-free welds and good mechanical properties.

One of the main issues that are yet to understand concerning dissimilar alloys welding is the possibility of operating a post-weld heat treatment (PWHT). The current literature suggests that a PWHT is often needed, in particular if the welded alloys are in the O state (Krishnan, 2002b; Malarvizhi & Balasubramanian, 2010; Priya et al., 2009; Chen et al., 2006; Sullivan & Robson, 2008). It is reported though that this kind of treatment can bring to grain growth and properties reduction, so that when aged alloys are welded, there is not yet total agreement on the best strategy to adopt.

In this work, we try to propose a method for the optimization of the post-weld heat treatment on joints of dissimilar alloys. This approach can be applied on any two precipitation-hardened alloys, and consists in the coupling of microscopic observations, Differential Scanning Calorimetry (DSC) analyses and hardness measurements in order to improve the overall performance of the weld, avoiding weak spots in specific locations of the weld.

Depending on the welding technique used, if LBW or FSW, the approach is slightly different, but the basic idea is the same. In LBW the fusion zone consists in the mixture of two or three different alloys, so that the standard treatments for the thermal aging of the base alloys can not be successfully used. By using composition analyses, DSC and microscopic observations, it is possible to determine the best thermal treatment for

increasing the hardness of the weld without incurring in over-ageing of either the base alloys or the weld itself.

In FSW no fusion zone is observed, however many modifications are observed in the HAZ, TMAZ and nugget. Starting from DSC analyses, that suggest the state of precipitates in the specific zones, it is possible to determine the best heat treatment temperature for the weld, and optimize its hardness.

In both cases, two factors are to consider: over-ageing that can occur in the HAZ as a result of the temperature increase during welding; limited increase of hardness in specific weld zones, due to microstructure modifications. It is important to find a compromise between the properties of the base alloys and the properties of the weld, to avoid weak spots in the whole system.

2. Characterization techniques

Samples were taken from the different weld zones by cutting: fusion zone, HAZ and base alloys for LBW; nugget, TMAZ, HAZ and base alloys for FSW.

Vickers or Brinell hardness was measured on polished cross-section of welded specimens, in the different zones of the weld and on base alloys. Microstructure was examined by optical microscopy and scanning electron microscopy. Compositional analysis of the different parts of the cross-section of the specimens was carried out by energy dispersive X-ray spectroscopy. Keller's reagent etching was sometimes used to improve the quality of optical microscopy observations.

Differential Scanning Calorimetry was used in order to identify the thermal phenomena occurring during a temperature scan between ambient temperature and 500 °C, at a heating rate of 20 °C/min and under flowing Ar atmosphere.

Indeed, DSC analysis has been frequently used to investigate the ageing sequence and the precipitation kinetics of several aluminium alloys (Mishra & Ma, 2005; Badini et al., 1990; Badini et al., 1995; Morgeneyer et al., 2006; Jena et al., 1989; Garcia Cordovilla & Louis, 1984; Garcia Cordovilla & Louis, 1991; Papazian, 1982; Genevois et al., 2005). The DSC analysis of solution treated aluminium alloys allows to observe during a temperature scan the precipitation sequence and the dissolution of precipitates. This is possible since the formation of the strengthening phases (GP zones, metastable intermediate precipitates and stable hardening phases) results in exothermal peaks while the precipitates dissolution is an endothermic phenomenon.

In the same manner DSC can be used to assess the state of a partially aged aluminium alloy. For instance, in the case of naturally aged specimens the peak relative to the GP zone formation is missing, and the peak concerning the formation of metastable precipitates is weakened. In the case of artificially aged specimens, both peaks are missing.

3. Results and discussion

The methodology proposed to analyse the behaviour of dissimilar alloys welds and to optimise their post-weld heat treatment (PWHT) is based on different steps:

- analysis of the behaviour of the base alloys;
- analysis of a weld between two parts of the same alloy (optional);
- analysis of the weld between dissimilar alloys;
- DSC analysis of samples taken from different parts of the weld;
- post-weld heat treatment and hardness measurement.

3.1 Laser beam welding

a. Preparation of the weld

Regarding LBW method, 2139 alloy and a 7000 series alloy with composition reported in Table 1 were welded. As a filler a 4047 alloy wire with 1 mm diameter was used. The 2139 alloy was furnished in 3.2 mm thick sheets, in the T8 temper (solution heat treated, quenched, cold worked, and aged at 175 °C for 16 h). The 7000 series alloy was used as 2.5 mm thick extrusion, in T4 temper (solution heat treated, quenched, naturally aged).

Alloy	Mean chemical composition (wt. %)									
	Si	Fe	Cu	Mn	Mg	Cr	Ti	Zn	Zr	Ag
2139	0.04	0.06	5.1	0.29	0.43	-	0.05	-	0.014	0.33
7xxx	0.10	0.11	0.61	0.15	3.1	0.15	0.02	10.0	0.10	-
4047	12.0	0.8	0.3	0.15	0.10	-	-	0.2	-	-

Table 1. Mean chemical composition of alloys used for LBW: 2139, 7xxx, 4047.

LBW has been performed using two continuous wave Nd:YAG lasers, with maximum laser power 4 kW and mixed argon and helium as shielding gas. T-shaped specimens were produced, and the chosen process parameters were: welding speed 6 m/min, wire feed rate 4.8 m/min, laser power 3.6 kW. The laser beam was focused on both sides of the contact surface between the two plates, using a 200 mm focusing lens and a 0.6 mm diameter focalized beam. Welded specimens were submitted to various artificial ageing treatments using an oil bath kept at constant temperature.

b. Analysis of the behaviour of the base alloys

In this case the analysis can be either experimental or based on the literature. The composition of the base alloys was already given in Table 1, while the mechanical properties of 7000 and 2139 alloys are reported in Table 2.

Alloy	Ultimate tensile strength (MPa)	Yield strength at 0.2% (MPa)	Fracture elongation (%)	Vickers hardness
2139-T8	480	435	12.5	150
7xxx-T4	660	550	8.9	190

Table 2. Mechanical properties of the alloys welded by laser beam: 2139, 7xxx.

c. Analysis of the weld of a single alloy

In the case of fusion-welded samples this step was not deemed necessary in order to study the weld between dissimilar alloys. In fact, the laser beam welding of two alloys with very different composition, adding a filler wire of a third alloy, brings to a material with a significantly different composition in the melted zone. Generally the weak spot in a LBW weld of a single alloy is between the weld and one of the base alloys, i.e. in the HAZ. However, when dissimilar alloys are considered, the alloy in the weld itself can become the weak spot due to the different composition and the lack of post-weld heat treatment (or due to an incorrect choice of temperature or time).

d. Analysis of the weld between dissimilar alloys

The first step in the analysis of the weld is a microstructure observation. In the case of the weld between 2139 and the 7000 series alloys, a compositional map of the weld is shown in

Figure 2, showing the different zones by their composition: 2139 alloy on the lower part of the image (less zinc), 7xxx alloy on the top (high zinc content) and melted zone in the middle (high silicon content).

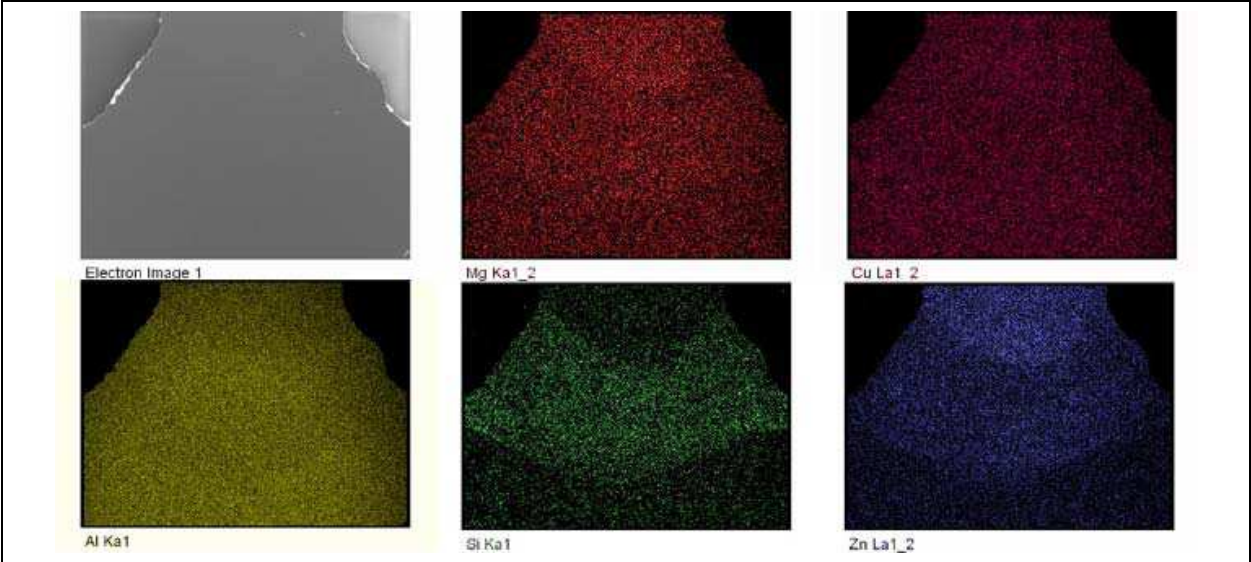


Fig. 2. Elemental map of a laser beam weld between 2139 (low) and 7xxx (high) alloys.

In Figure 3 the microstructure of different parts of the welds is shown. Hot cracks are not observed in the weld, and porosity is rare. The microstructure of 2139 alloy shows almost equiaxed grains, while 7000 series alloy shows the elongated grains typical of extruded structures. In the molten zone a very fine microstructure is observed, with small equiaxed grains. A small fraction of precipitates can be observed at grain boundaries. HAZ zones present a rather sharp transition between base alloy and fusion zone. The precipitates assume partially oriented features.

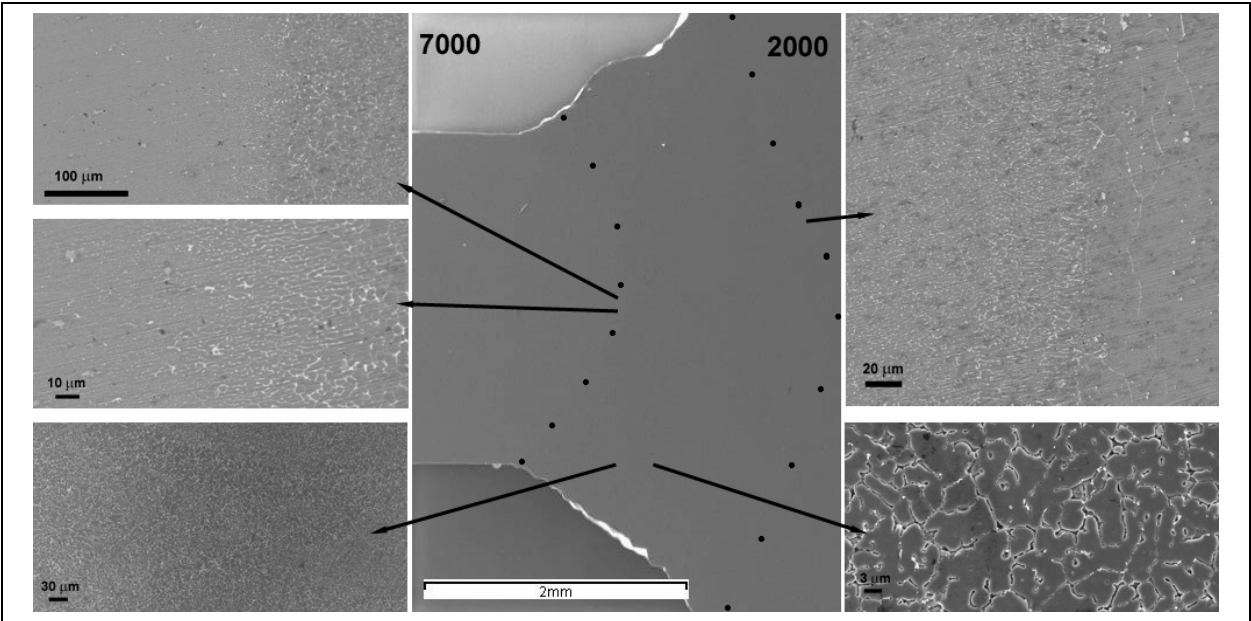


Fig. 3. Microstructure of a laser beam weld between 2139 (right) and 7xxx (left) alloys.

A hardness map of the weld is shown in Figure 4. It is evident that the lowest hardness is observed in the weld zone.

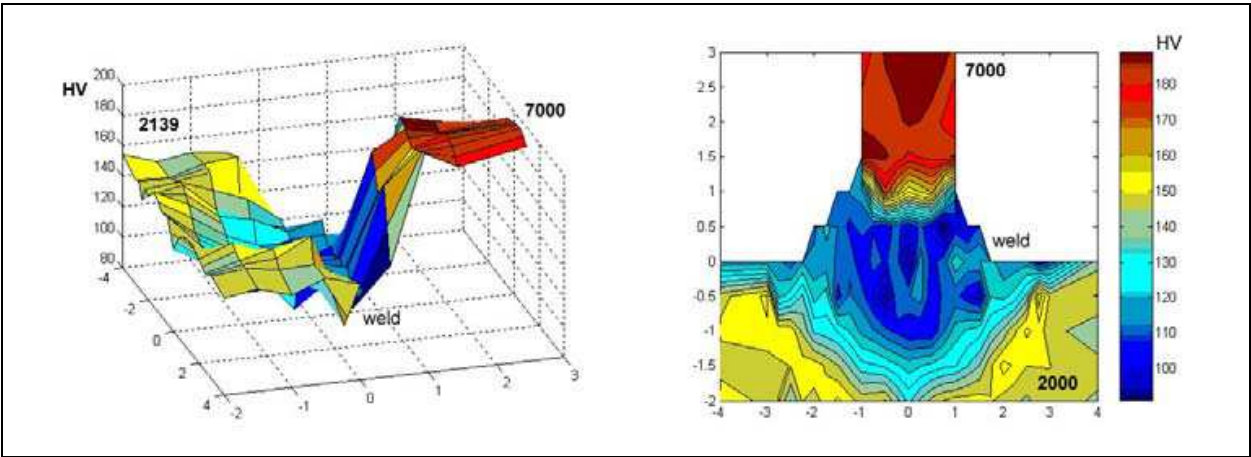


Fig. 4. Hardness map of a laser beam weld between 2139 and 7xxx alloys.

e. DSC analysis of samples taken from different parts of the weld

In the case of LBW, samples were taken from base alloys, from the HAZs, and from the fusion zone. Figure 5 shows the DSC curves for the 7000 series alloy and the fusion zone. The HAZ zones were too small to observe effects by DSC, so that measurements did not reveal further information on the HAZs. The DSC curve of 2139 alloy was flat, due to the fact that this alloy had been already submitted to heat treatment before welding. The DSC experiments show, in the case of 7000 alloy, a endothermic peak due to precipitates dissolution, starting close to 100 °C, followed by a double exothermic peak, corresponding to the precipitation of intermetallic phases. The onsets of the two peaks are around 160-180 °C and close to 200 °C. A third exothermic peak is observed at higher temperature, close to 250 °C. The fusion zone presents no endothermic signal (due to lack of a significant quantity of precipitates), a small exothermic peak starting at 170 °C and a large exothermic peak starting at 200 °C.

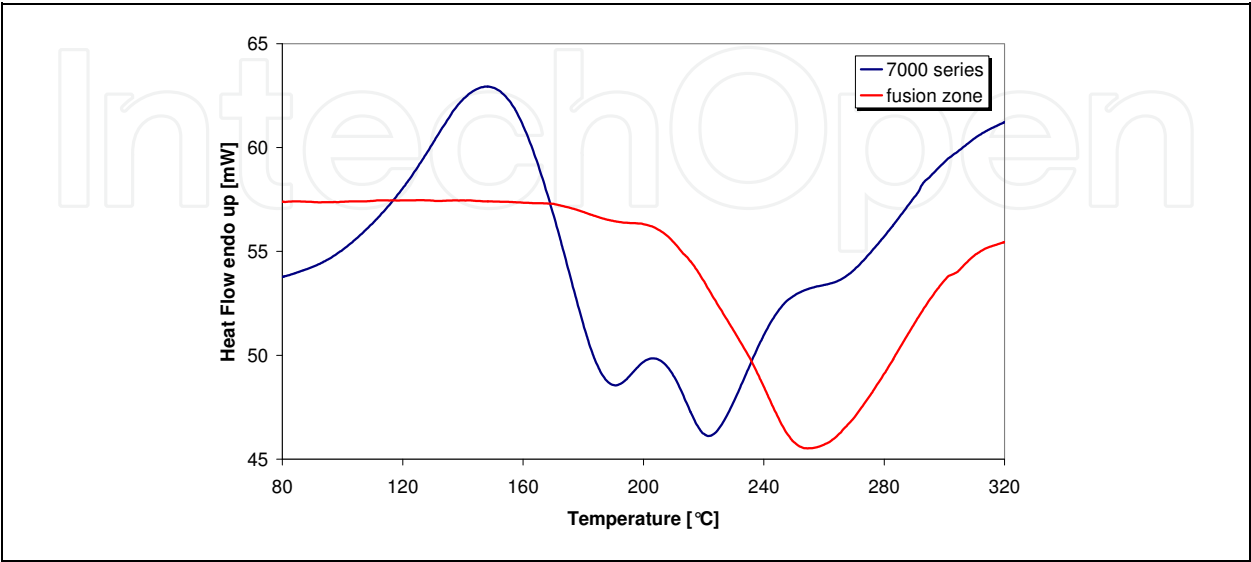


Fig. 5. DSC curves of the 7xxx alloy and of the fusion zone.

From these data a convenient thermal treatment temperature must be chosen. Since ageing must not be carried out too far, to avoid excessive growth of precipitates, the temperature must be kept relatively low. For this reason in this case 170 °C was chosen as the heat treatment temperature. The peak of the fusion zone is starting right around this temperature, so that precipitation of strengthening phases is forecast.

f. Post-weld heat treatment and hardness measurement

A PWHT was performed by varying the time of the heat treatment in the range 0-18 hours, and microhardness measurements were performed on the obtained samples. The results are shown in Figure 6.

While the 2139 alloy maintains a constant hardness during heat treatment, the measurements demonstrates a significant increase in hardness over a limited time range for both 7000 alloy and fusion zone. An excessive permanence at high temperature brought to over-ageing in both zones. The choice of heat treatment time then is limited to 6 to 10 hours. In the former case (6 hours) the weld remains less hardened but the 7000 alloy does not go into over-ageing. In the latter (10 hours) the 7000 alloy becomes slightly over-aged but the weld receives the best hardening treatment.

The approach based on the DSC measurements allowed thus to determine a convenient temperature for heat treatment. A higher temperature would bring to fast over-ageing of the weld, while a lower temperature would not guarantee a sufficient aging to grant the best mechanical properties. This was demonstrated by heat treating the alloys at 140 °C, far from the DSC peaks. Even if the 7xxx alloy showed an increase in hardness during this heat treatment, the weld hardness remained low, suggesting no improvement in its mechanical properties.

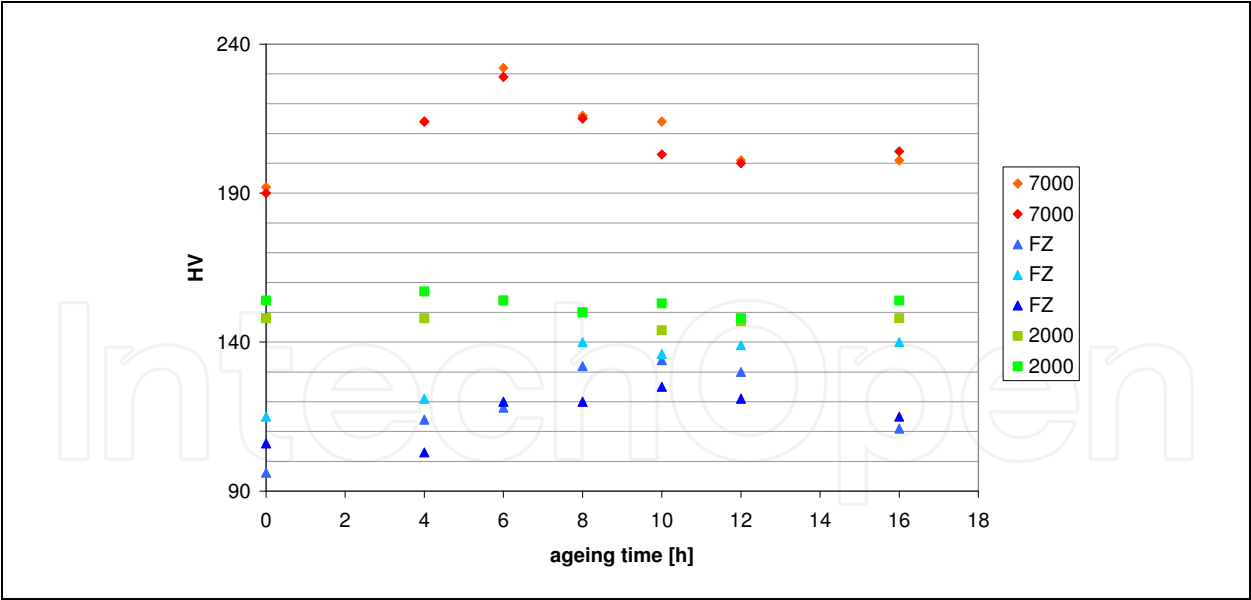


Fig. 6. Hardness of the various parts of the weld after the post-weld heat treatment.

3.2 Friction stir welding

a. Preparation of the weld

Regarding FSW samples, three alloys were used in the form of 3.1 mm thick sheets: 2198 alloy in T3 temper (solution heat treated, quenched, cold worked, and naturally aged), 6013

alloy in T4 temper (solution heat treated, quenched, naturally aged), 7475 alloy in W state (solution heat treated, quenched). The composition of the three alloys is given in Table 3.

Alloy		Si	Fe	Cu	Mn	Mg	Cr	Ti	Zn	Zr	Ag	Li	other
2198	min	0	0	2.9	0	0.25	0	-	0	0.04	0.10	0.80	-
	max	0.08	0.10	3.5	0.50	0.80	0.05	-	0.35	0.18	0.50	1.10	-
7475	min	0	0	1.2	0	1.9	0.18	0	5.2	-	-	-	0
	max	0.1	0.12	1.9	0.06	2.6	0.25	0.06	6.2	-	-	-	0.15
6013	min	0.6	0	0.6	0.2	0.8	0	0	0	-	-	-	0
	max	1.0	0.5	1.1	0.8	1.2	0.1	0.1	0.25	-	-	-	0.15

Table 3. Mean chemical composition of alloys used for FSW: 2198, 7475, 6013.

Two kinds of weld were considered in this work: the first between two 6013 plates; the second between 2198 and 7475 alloys. The welding was performed by using a tool with a nib 3.2 mm long and with 4.7 mm diameter, and a shoulder with diameter of 13.4 mm. A milling machine Rigiva RS 100 was used for welding the sheets in the direction perpendicular to the rolling direction. The work conditions were welding speed from 50 to 200 mm/min, pin rotation speed 830 rpm and tilt angle of the tool 2°.

Welded specimens were submitted to various artificial ageing treatments using an oil bath kept at constant temperature.

b. Analysis of the behaviour of the base alloys

The base alloys are well-known, so that composition and mechanical data were taken from the literature. Mechanical data of the three alloys are given in Table 4.

Alloy	Ultimate tensile strength (MPa)	Yield strength at 0.2% (MPa)	Fracture elongation (%)	Vickers hardness
2198 T3	370	275	15	100
7475 T761	525	460	12	160
6013 T4	320	220	20	100
6013 T6	395	355	12	135

Table 4. Mechanical properties of the alloys welded by laser beam: 2198, 7475, 6013.

The 6013 T4 alloy has been shown to contain Si, GP zones and $\alpha(\text{AlFeMnSi})$ (probably of $(\text{Fe,Mn})_3\text{Si}_x\text{Al}_{12}$ composition), with the development of Mg_2Si (β'') and $\text{Al}_4\text{Cu}_2\text{Mg}_8\text{Si}_7$ (Q') precipitates during ageing at 180 °C (Barbosa et al., 2002; Genkin, 1994). Mg_2Si precipitates are also known to grow from needle-shape to rod-shape and finally to plate-shape (Heinz & Skrotzki, 2002). The passage from T4 to T6 brings to an increase of mechanical performance, in particular of yield strength, that has been motivated with the simultaneous presence of β'' and Q' precipitates. Thus, a typical heat treatment for 6013 alloy is a T6, at 180-190 °C for a few hours.

In 7475 alloy the typical precipitates are MgZn_2 (η or η') and CuMgAl_2 S phase (Norman et al., 2003). The mechanical data of 7475 alloy were given in the T761 state since it is one of the most common state for this alloy. Moreover, after heat treatment the mechanical properties are heavily altered from those of W state, so that properties of the aged alloys are more interesting for comparison. Heat treatment is generally performed in two steps at around 120 and 180 °C (Li et al., 2007).

The main precipitates in 2198 alloys aged at 155 °C are Al_2CuLi (T1), then Al_3Li (δ') and Al_2CuMg (S'), sometimes Al_2Cu , with formation of small AlLi and Al_3Zr quantities (Cavaliere et al., 2009; Decreus et al., 2010; Chen et al., 2010). Moreover, lithium allows for a reduction of weight (roughly 3% reduction every 1% of Li in the alloy).

c. Analysis of the weld of a 6013 alloy

The case of the welding of 6013 alloy will be considered as an example of the procedure that can be brought out to study the effect of welding on the properties of the alloy. Indeed, there is no real difference between the case of a single alloy weld and that of a dissimilar weld. The image of the 6013-6013 weld is shown in Figure 7.

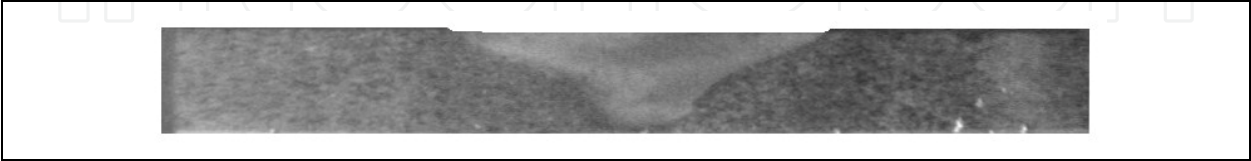


Fig. 7. Image of the weld between two 6013 alloy plates.

On Figure 8 are presented instead the Brinell and Vickers hardness curves for the weld. It is evident that the lower hardness is present on the retreating side of the weld, at the interface between TMAZ and HAZ.

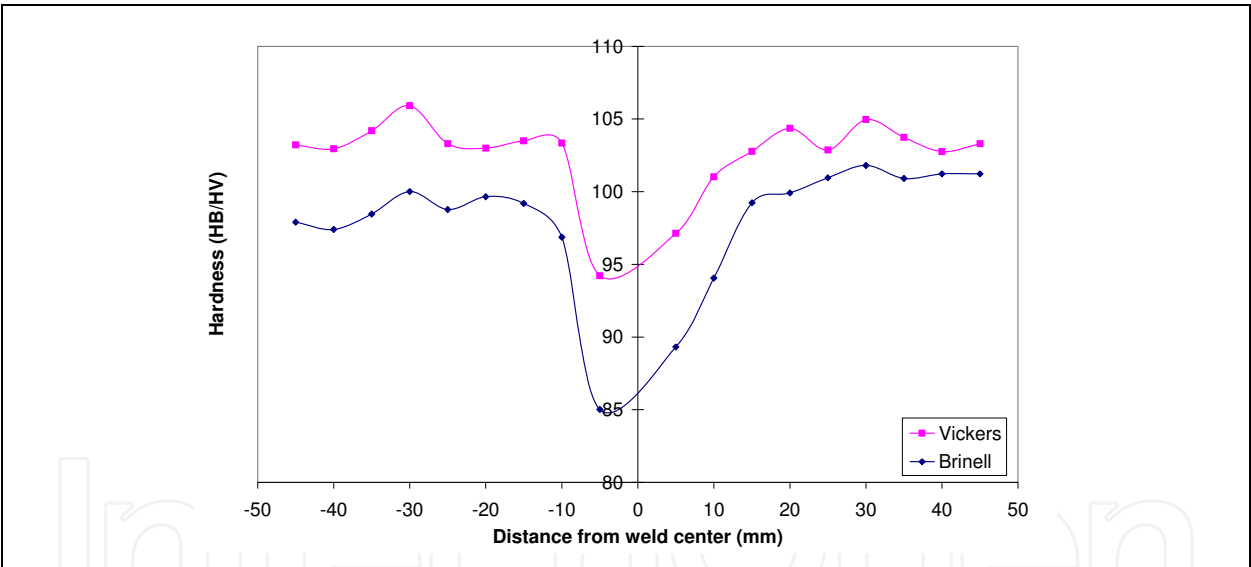


Fig. 8. Brinell and Vickers hardness profiles for a 6013-6013 weld.

On Figure 9 is presented the DSC curves for samples taken at different positions along the weld.

The curves show clearly how at +30 mm and -30 mm from the weld centre the 6013 alloy is in the unmodified T4 state. On heating an endothermic peak is observed typical of GP zones dissolution, around 160 °C, followed by three peaks for the precipitation of strengthening phases. At +10 and -10 mm from the weld centre, only a hint of the endothermic peak is observed, suggesting that GP zones dissolution already took place during the welding treatment, due to the increase of temperature. However the three peaks linked to precipitation are yet observed. At +5 and -5 mm, i.e. very close to the heavily deformed zone, only the exothermic precipitation peaks are observed. There is a small shift of the main

peak toward lower temperature, with the second and third precipitation peaks disappeared or extremely low. In the nugget the main exothermic peak is wider and shifted toward lower temperature. This suggest that in this zone a finer microstructure is present, as confirmed by microscopic observations (Figure 10), and/or higher residual stresses, that brings to an easier precipitation of strengthening phases.

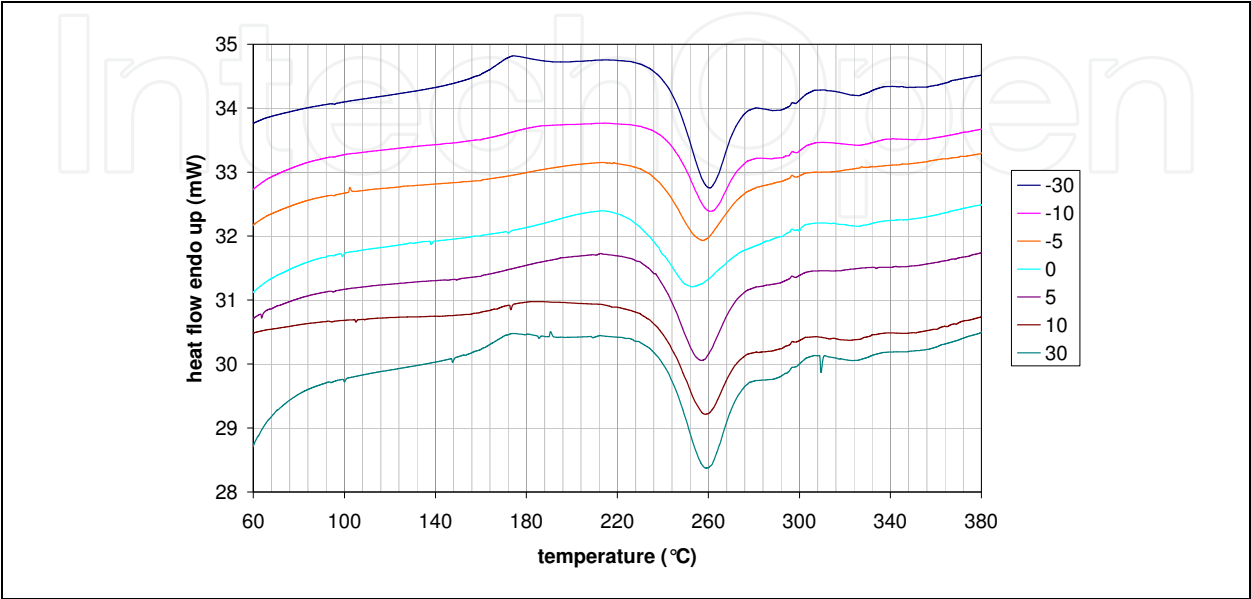


Fig. 9. DSC curves for different parts of a 6013-6013 weld.

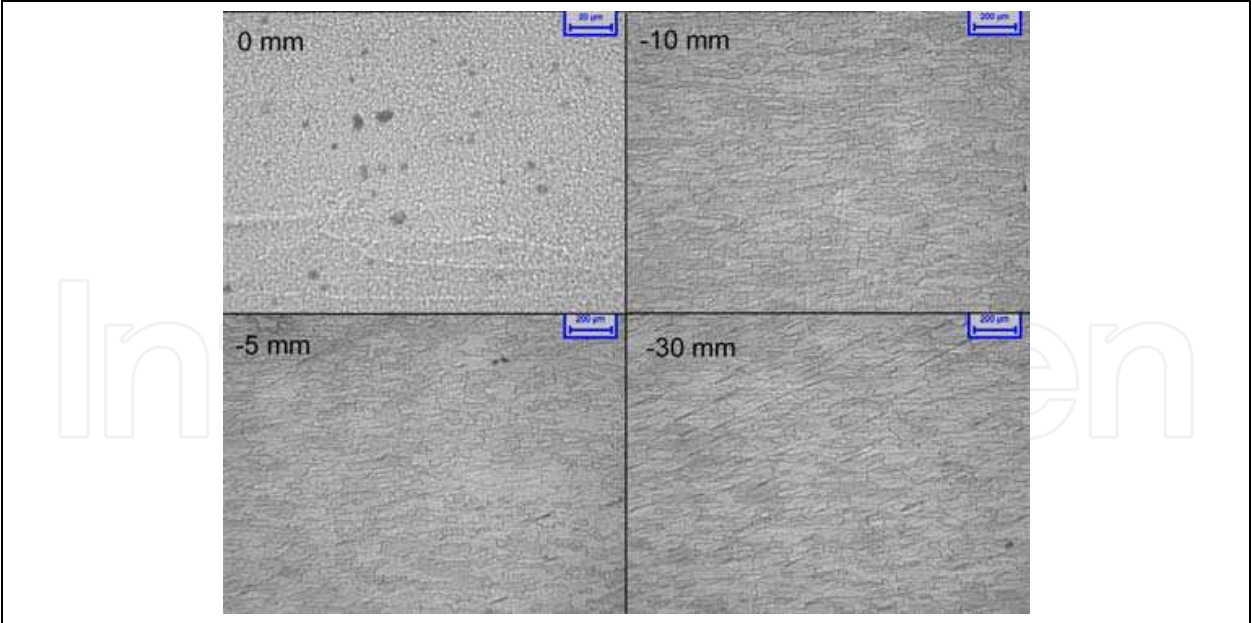


Fig. 10. Microstructure of different parts of a 6013-6013 weld.

DSC analysis thus allows to roughly determine the state of the different parts of the weld, suggesting that for 6013 alloy precipitation must yet occur, so that a significant increase of hardness by PWHT can be obtained. As said before, 6013 alloys are generally heat treated at 180-190 °C for a few hours. The DSC trace shows that these temperature are quite far from

the main precipitation peak, however DSC experiments made on heat treated samples demonstrate that a partial precipitation already occurs, probably with very small β'' and Q' precipitates (Barbosa et al., 2002). Figure 11 shows the DSC curves for welded samples aged at 160 (18 h) and 190 °C (3 h).

It is evident that the intensity of the exothermic peak is much lower than the intensity before heat treatment. This suggests that precipitation occurred during heat treatment. The effect of precipitation can be observed in the hardness curves of Figure 12.

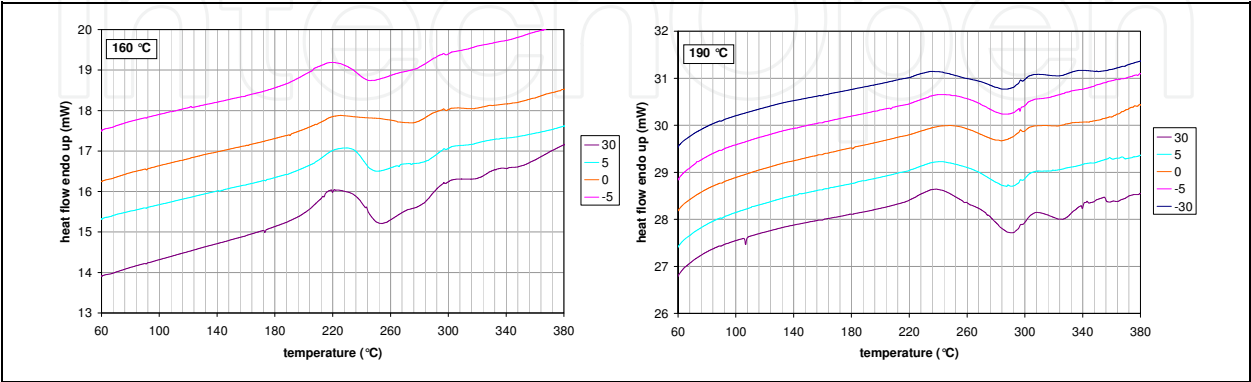


Fig. 11. DSC curves for different parts of a 6013-6013 weld after 160 °C and 190 °C heat treatments.

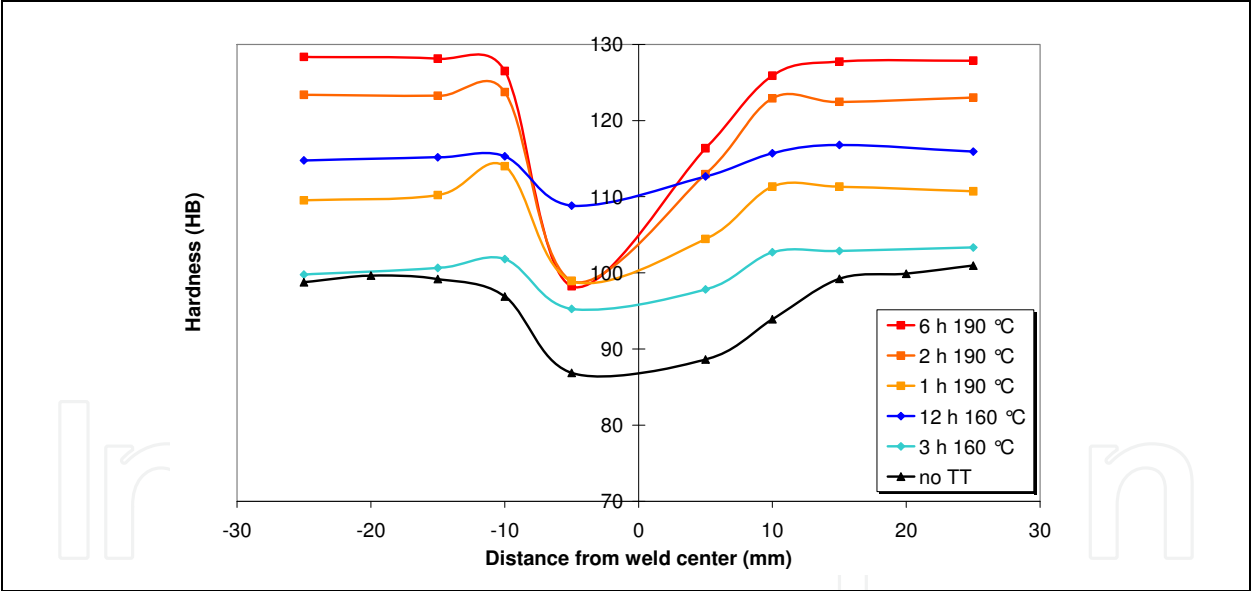


Fig. 12. Hardness profiles for a 6013-6013 weld after 160 °C and 190 °C heat treatments.

Figure 12 shows how the temperature of heat treatment heavily influences the behaviour of both base alloys and weld. Depending on the temperature of the heat treatment, different hardness profiles can be observed. If this heat treatment is kept at low temperature a lower increase of hardness of base alloys occurs, but a larger increase of hardness in the HAZ. If the heat treatment is made at higher temperatures, the precipitates growth prevails and no hardness increase in the weld is observed. In this last conditions, the marked improvement in hardness of the base metals risk to be overcome by the low resistance of the weld zone.

d. Analysis of the weld between dissimilar alloys

The case of welding between 7475 and 2198 will be presented for the welding of dissimilar alloys. An image of the weld is shown in Figure 13.

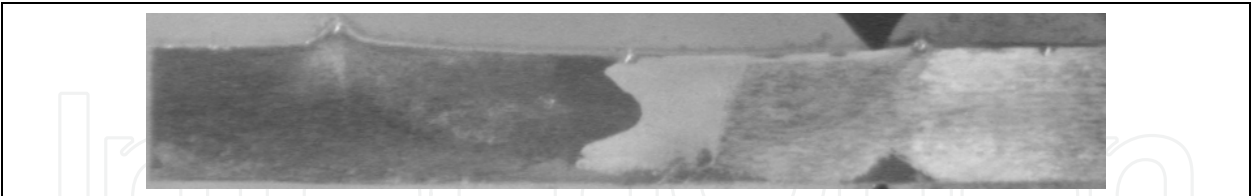


Fig. 13. Image of the weld between 2198 and 7475 alloy plates.

From the DSC curves of pure 2198 alloy (Figure 14) it can be seen that, passing from T3 state to solubilized one, a less marked exothermic precipitation is observed, and a higher temperature is required for the formation of the strengthening phases. This is probably due to the elimination of cold working effect thanks to the solution heat treatment.

In the case of the dissimilar weld (Figure 15), curves for +30 mm from the weld (retreating side, 7475 alloy) are very similar to curves of the pure 7475 alloy, and the same happens for -30 mm (advancing side, 2198 alloy). The behaviour of the 7475 alloy side is quite constant for samples took on HAZ and TMAZ zones, showing only a smaller peak than the base alloy, linked to a partial precipitation of phases due to the high temperature suffered during welding.

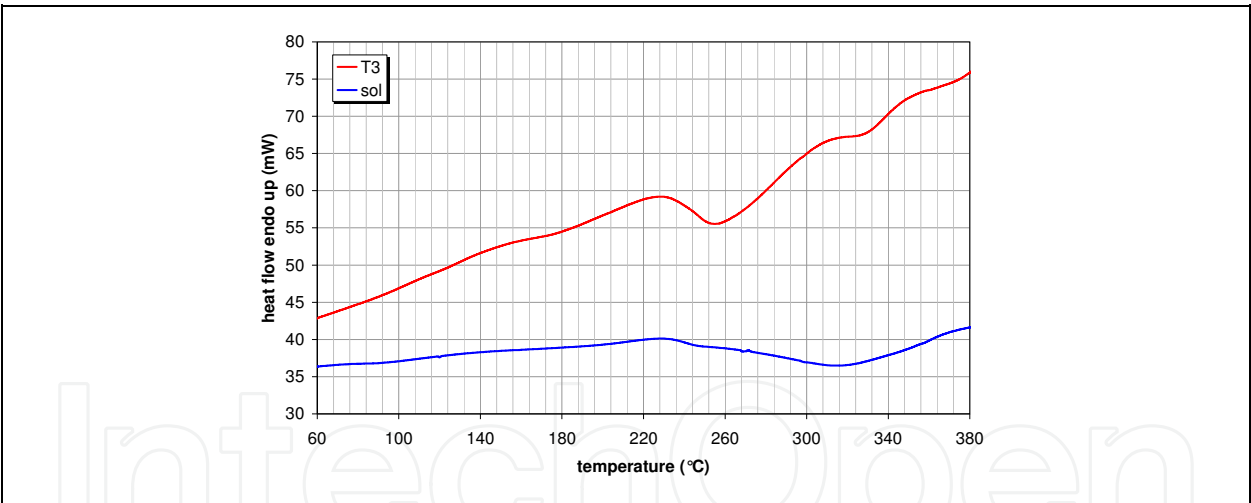


Fig. 14. DSC curves for 2198 alloy.

In the nugget, a behaviour similar to that of the 7475 alloy is observed, with a small precipitation peak. From the 2198 side, the effect of the high temperature developed during the welding is to eliminate the effect of the cold working, so that at -5 mm the curve is similar to the one of solution heat treated 2198 alloy. At -10 mm a peak is yet observed, even if shifted toward higher temperature with respect to the base alloy.

Due to the different approach needed to age the 2198 and the 7475 alloys, different temperatures were tested also for a 2198-2198 weld, in order to understand the effect of temperature on the strengthening mechanism. At low temperature (155 °C) welds need very long times to reach good hardness values, as in the case of 6013 alloy. At high temperature (200 °C) the maximum hardness is reached in 3-4 hours (Figure 16).

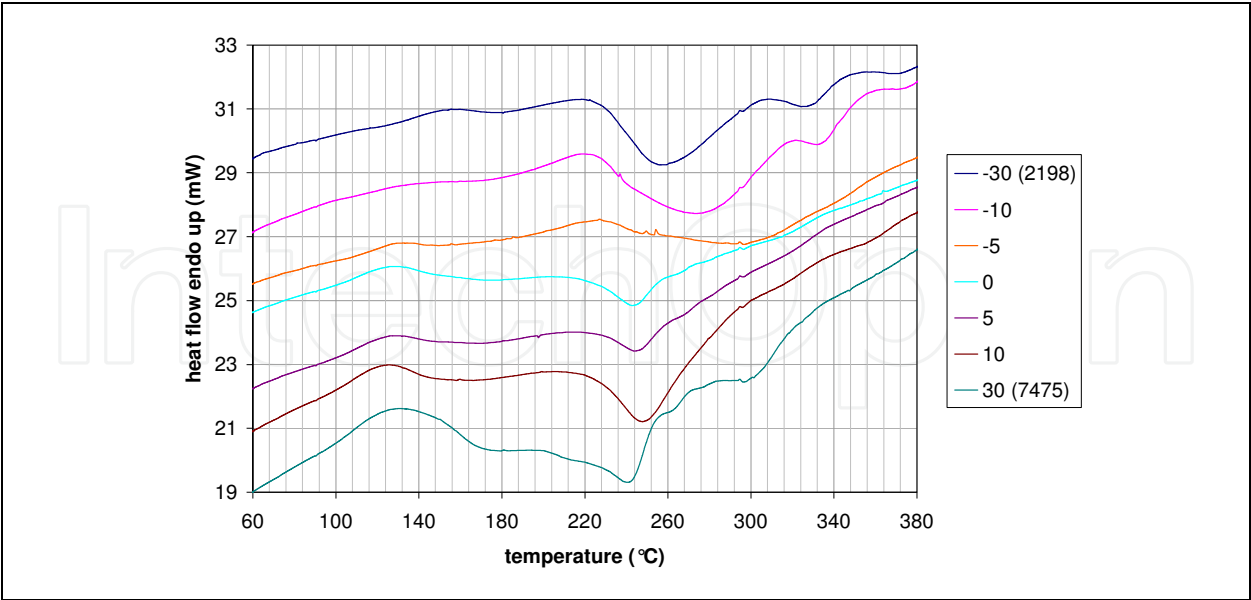


Fig. 15. DSC curves for different parts of a 2198-7475 weld.

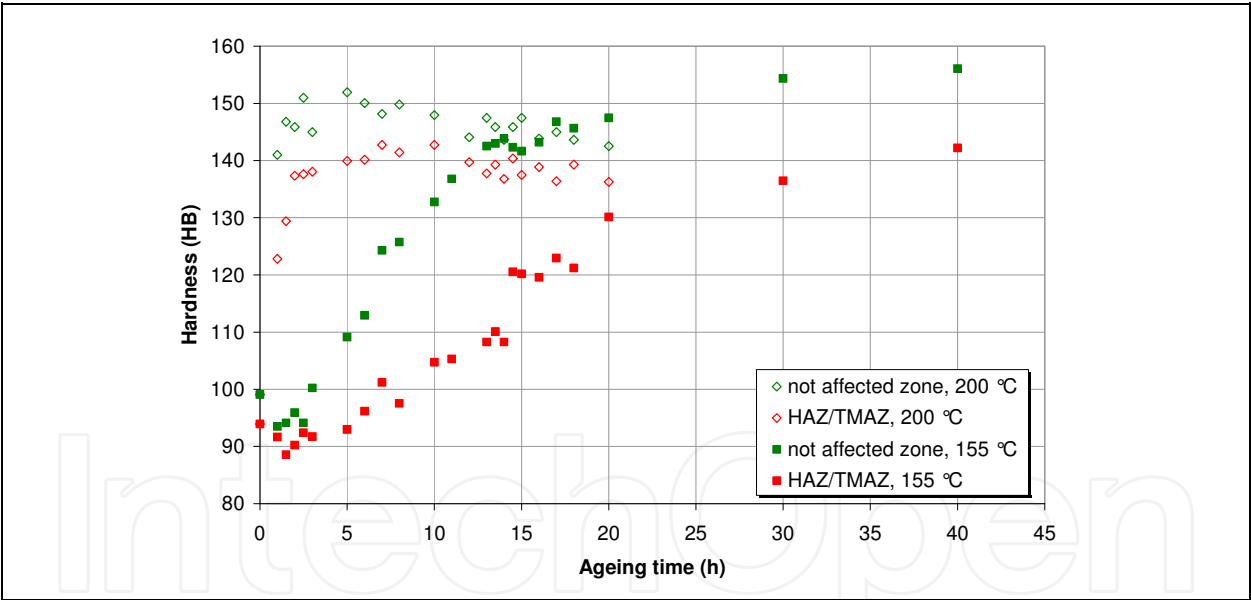


Fig. 16. Hardness curves of different parts of a 2198-2198 weld after 155 °C and 200 °C heat treatments.

The ageing of 7475 alloy is generally realised in a two-step fashion, with a high temperature step at 170-180 °C. The curve showing the behaviour of a 7475-7475 weld is shown in Figure 17.

The risk of over-ageing is rather evident, however it must be stressed that the weak spot in a welded structure is often the weld. For this reason it was chosen to provide an increase of hardness for the 2198 HAZ/TMAZ zone and suffer a small over-ageing of the 7475 alloy. The curve on Figure 18 shows the ageing curve for 2198-7475 weld.

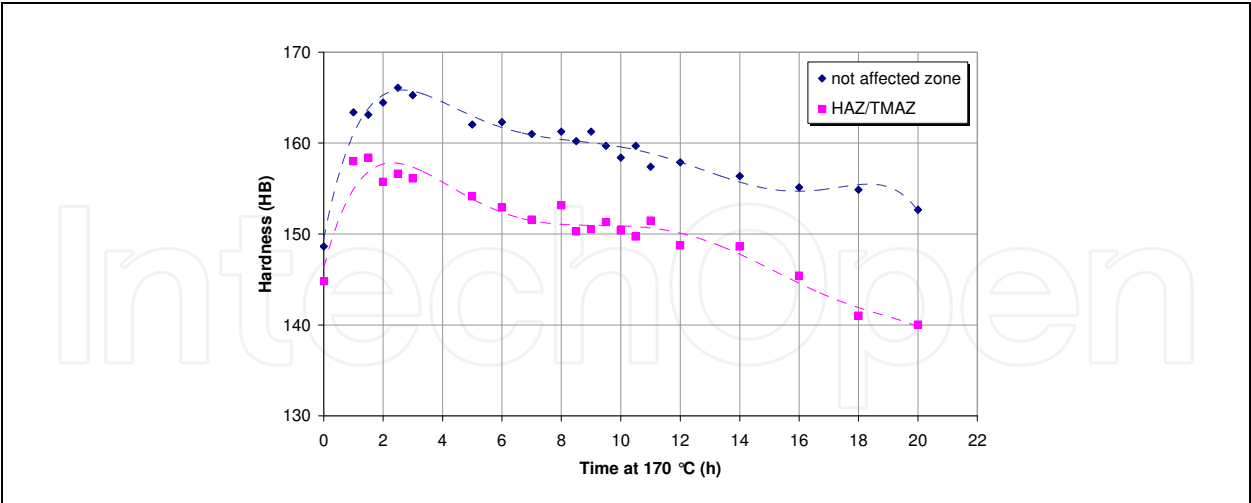


Fig. 17. Hardness curves of different parts of a 7475-7475 weld after heat treatment.

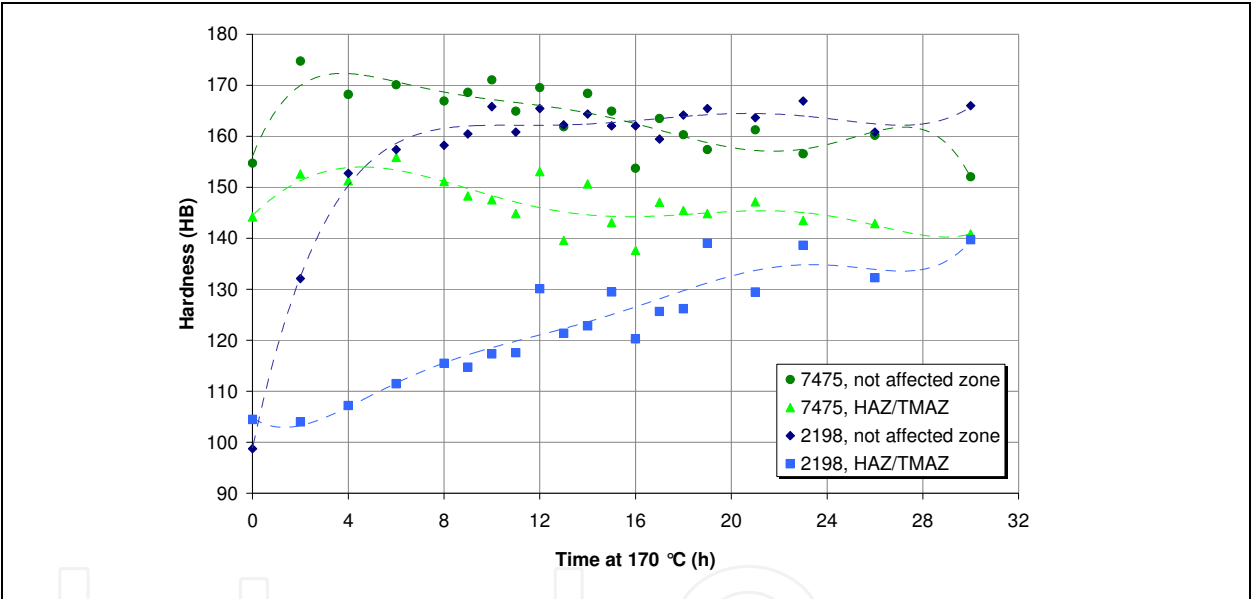


Fig. 18. Hardness curves of different parts of a 2198-7475 weld after heat treatment.

It is evident that while over-ageing is slowly occurring on the base 7475 alloy, precipitation is happening in the weld, with a significant hardening effect, that remains very low in the zone for optimal ageing of the only 7475 alloy.

DSC curves confirm that precipitation occurred, as shown in Figure 19. No significant peak was detected after ageing.

Thus, post welding heat treatments are able to improve mechanical properties of the welds, if the ageing conditions are carefully controlled. The use of the standard ageing treatments used for the base alloys that have been welded not always provide the best results, neither for similar alloys welding nor for dissimilar ones. The control of the PWHT is essential for avoiding weak spots in the weld, that can lower substantially the mechanical properties of the whole welded system.

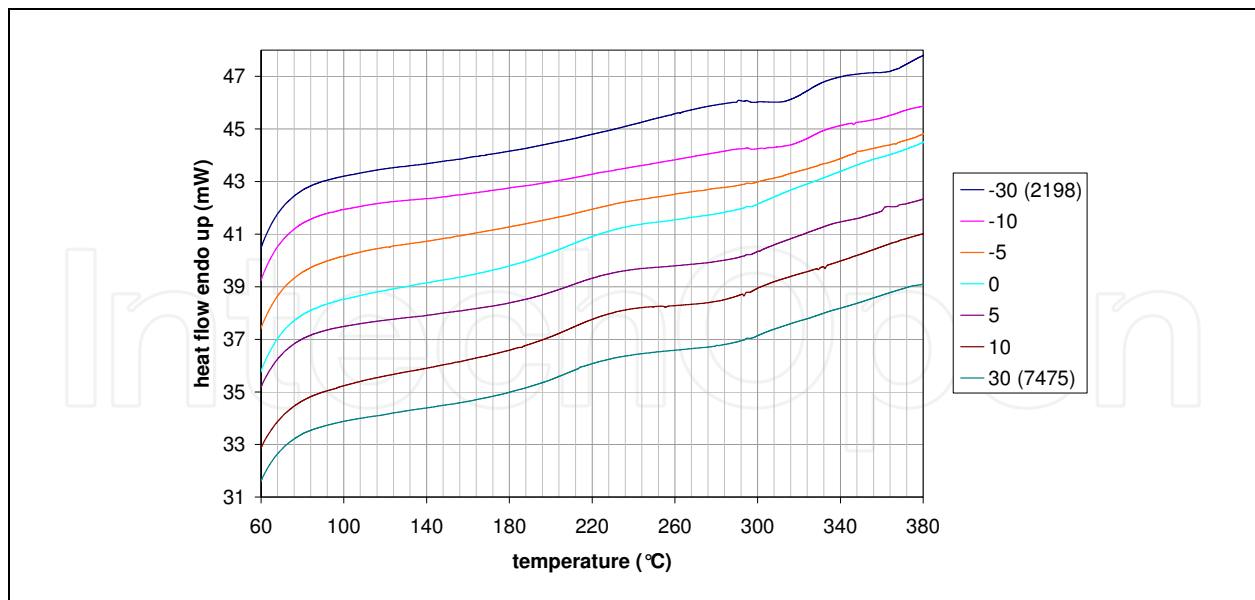


Fig. 19. DSC curves for different parts of a 2198-7475 weld after heat treatment.

4. Conclusion

In this work a method for the study of the ageing behaviour of laser beam or friction stir welds between similar or dissimilar alloys is presented. The approach is based on the DSC study of different parts of the weld. Coupling DSC measurements with literature data, it is possible to choose a convenient heat treatment to optimize the hardness profile of the weld. In most of the cases, a compromise must be found between the improvement of the weld properties and that of the base alloys. A laser beam weld of dissimilar alloys 2139 and 7xxx showed a marked increase in hardness for the weld, at expense of a slight over-ageing of the 7xxx alloy. In the case of the friction stir welding of a 6013-6013 system, a lower temperature than the standard one for the heat treatment of the alloy gives the best results, bringing to a slower yet more uniform hardness increase in the weld. Finally, in a 2198-7475 weld the permanence at high temperature must be carefully regulated: if a short time is chosen, the weld does not harden enough; if too long a time is selected, an important over-ageing of the 7475 alloy occurs.

5. References

- Badini, C.; Marino, F. & Tomasi, A. (1990). DSC study of ageing sequence in 6061 aluminum alloy-SiC whiskers composite. *Mater. Chem Phys.*, 25, 1, 57-70, 0254-0584
- Badini, C.; Marino, F. & Verné, E. (1995). Calorimetric study on precipitation path in 2024 alloy and its SiC composite. *Mater. Sci. Eng. A*, 191, 1-2, 185-191, 0921-5093
- Badini, C., Pavese, M., Fino, P. & Biamino, S. (2009). Laser beam welding of dissimilar aluminium alloys of 2000 and 7000 series: effect of post-welding thermal treatments on T joint strength. *Sci. Technol. Weld. Join.*, 14, 6, 484-492, 1362-1718
- Barbosa, C; Rebello, J. M. A.; Acselrad, O.; Dille, J. & Delplancke J.-L. (2002). Identification of precipitates in 6013 aluminum alloy (Al-Mg-Si-Cu). *Z. Metallkd.*, 93, 3, 208-211
- Benavides, S.; Li, Y.; Murr, L. E.; Brown, D. & McClure, J. C. (1999). Low-temperature friction stir welding of 2024 aluminium. *Scripta Mater.*, 41, 8, 809-15, 1359-6462

- Braun, R. (2006). Nd:YAG laser butt welding of AA6013 using silicon and magnesium containing filler powders. *Mater. Sci. Eng. A*, 426, 1-2, 250-262, 0921-5093
- Buffa, G.; Donati, L.; Fratini, L. & Tomesani, L. (2006). Solid state bonding in extrusion and FSW: Process mechanics and analogies. *J. Mater. Process. Technol.*, 177, 1-3, 344-347, 0924-0136
- Cavaliere, P.; Cabibbo, M.; Panella, F. & Squillace, A. (2009). 2198 Al-Li plates joined by Friction Stir Welding: Mechanical and microstructural behaviour. *Mater. Des.*, 30, 9, 3622-3631, 0261-3069
- Charit, I. & Mishra, R. S. (2003). High strain rate superplasticity in a commercial 2024 Al alloy via friction stir processing. *Mater. Sci. Eng. A*, 359, 1-2, 290-296, 0921-5093
- Chen, J.; Madi, Y.; Morgeneyer, T. F. & Besson, J. (2010). Plastic flow and ductile rupture of a 2198 Al-Cu-Li aluminum alloy. *Comput. Mater. Sci.*, in press, DOI: 10.1016/j.commatsci.2010.06.029
- Chen, Y. C.; Liu, H. J. & Feng, J. C. (2006). Effect of post-weld heat treatment on the mechanical properties of 2219-O friction stir welded joints. *J. Mater. Sci.*, 41, 1, 297-299, 0022-2461
- Cicala, E.; Duffet, G.; Andrzejewski, H.; Grevey, D. & Ignat, S. (2005). Hot cracking in Al-Mg-Si alloy laser welding - Operating parameters and their effects. *Mater. Sci. Eng. A*, 395, 1-2, 1-9, 0921-5093
- Decreus, B.; Deschamps, A. & Donnadieu, P. (2010). Understanding the mechanical properties of 2198 Al-Li-Cu alloy in relation with the intra-granular and inter-granular precipitate microstructure. *J. Phys.: Conf. Ser.* 240, 012096, 1742-6596
- Derry, C. G. & Robson, J. D. (2008). Characterisation and modelling of toughness in 6013-T6 aerospace aluminium alloy friction stir welds. *Mater. Sci. Eng. A*, 490, 1-2, 328-334, 0921-5093
- Di, S.; Yang, X.; Luan, G. & Jian, B. (2006). Comparative study on fatigue properties between AA2024-T4 friction stir welds and base materials. *Mat. Sci. Eng. A*, 435-436, 389-395, 0921-5093
- Dubourg, L.; Merati, A. & Jahazi, M. (2010). Process optimisation and mechanical properties of friction stir lap welds of 7075-T6 stringers on 2024-T3 skin. *Mater. Des.*, 31, 7, 3324-3330, 0261-3069
- Fratini, L.; Pasta, S. & Reynolds, A. P. (2009). Fatigue crack growth in 2024-T351 friction stir welded joints: Longitudinal residual stress and microstructural effects. *Int. J. Fatigue*, 31, 3, 495-500, 0142-1123
- Garcia Cordovilla, C. & Louis, E. (1984). Characterization of the microstructure of a commercial Al-Cu alloy (2011) by differential scanning calorimetry (DSC). *J. Mater. Sci.*, 19, 1, 279-290, 0022-2461
- Garcia Cordovilla, C. & Louis, E. (1991). A differential scanning calorimetry investigation of the effects of zinc and copper on solid state reactions in Al-Zn-Mg-Cu alloys. *Mater. Sci. Eng. A*, 132, 1-2, 135-141, 0921-5093
- Genevois, C.; Deschamps, A.; Denquin, A. & Doisneau-Cottignies, B. (2005). Quantitative investigation of precipitation and mechanical behaviour for AA2024 friction stir welds. *Acta Mater.*, 53, 8, 2447-2458, 1359-6454
- Genkin, J.-M. P. (1994). Corrosion fatigue performance of Alloy 6013-T6. *Master Degree, Massachusetts Institute of Technology*, February 1994, MIT, Boston

- Hamilton, C.; Dymek, S. & Sommers A. (2008). A thermal model of friction stir welding in aluminum alloys. *Int. J. Mach. Tools Manuf.*, 48, 10, 1120-1130, 0890-6955
- Hatamleh, O.; Rivero, I. V. & Maredia, A. (2008). Residual Stresses in Friction-Stir-Welded 2195 and 7075 Aluminum Alloys. *Metall. Mater. Trans. A*, 39, 12, 2867-2874, 1073-5623
- Heinz, B. & Skrotzki, B. (2002). Characterization of a Friction-Stir-Welded Aluminum Alloy 6013. *Metall. Mater. Trans. B*, 33, 3, 489-498, 1073-5615
- Hirasawa, S.; Badarinarayan, H.; Okamoto K.; Tomimura T. & Kawanami T. (2010). Analysis of effect of tool geometry on plastic flow during friction stir spot welding using particle method. *J. Mater. Process. Technol.*, 210, 11, 1455-1463, 0924-0136
- Jata, K. V., Sankaran, K. K. & Ruschau, J. J. (2000). Friction-stir welding effects on microstructure and fatigue of aluminum alloy 7050-T7451. *Metall. Mater. Trans. A*, 31, 9, 2181-2192, 1073-5623
- Jena, A. K.; Gupta, A. R. & Chaturvedi, M. C. (1989). A differential scanning calorimetric investigation of precipitation kinetics in the Al-1.53 wt%Cu-0.79wt%Mg alloy. *Acta Metall.*, 37, 3, 885-895
- Krishnan, K. N. (2002a). On the formation of onion rings in friction stir welds. *Mater. Sci. Eng. A*, 327, 2, 246-251, 0921-5093
- Krishnan, K. N. (2002b). The effect of post weld heat treatment on the properties of 6061 friction stir welded joints. *J. Mater. Sci.*, 37, 3, 473-480, 0022-2461
- Kroninger, H. R. & Reynolds, A. P. (2002). R-curve behaviour of friction stir welds in aluminium-lithium alloy 2195. *Fatigue Fract. Eng. Mater. Struct.*, 25, 3, 283-290, 8756-758X
- Kwon, Y. J.; Shigematsu, I. & Saito, N. (2003). Mechanical properties of fine-grained aluminum alloy produced by friction stir process. *Scripta Mater.*, 49, 8, 785-789, 1359-6462
- Kwon, Y. J.; Shigematsu, I. & Saito N. (2008). Dissimilar friction stir welding between magnesium and aluminum alloys. *Mater. Letters*, 62, 23, 3827-3829, 0167-577X
- Lee, W.-B.; Yeon, Y.-M. & Jung, S.-B. (2003). The joint properties of dissimilar formed Al alloys by friction stir welding according to the fixed location of materials. *Scripta Mater.*, 49, 5, 423-428, 1359-6462
- Li, H.; Geng, J.; Dong, X.; Wang, C. & Zheng, F. (2007). Effect of Aging on Fracture Toughness and Stress Corrosion Cracking Resistance of Forged 7475 Aluminum Alloy. *J. Wuhan Univ. Technol. Mater. Sci. Ed.*, June 2007, 191-195, 1000-2413
- Mahoney, M. W.; Rhodes, C. G.; Flintoff, J. G.; Spurling, R. A. & Bingel, W. H. (1998). Properties of friction-stir-welded 7075 T651 aluminum. *Metall. Mater. Trans. A*, 29, 7, 1955-1964, 1073-5623
- Malarvizhi, S. & Balasubramanian, V. (2010). Effects of Welding Processes and Post-Weld Aging Treatment on Fatigue Behavior of AA2219 Aluminium Alloy Joints. *J. Mater. Eng. Perform.*, in press, DOI: 10.1007/s11665-010-9682-5
- Mendez, P. F.; Tello, K. E. & Lienert T. J. (2010). Scaling of coupled heat transfer and plastic deformation around the pin in friction stir welding. *Acta Mater.*, 58, 6012-6026, 1359-6454
- Mishra, R. S. & Ma, Z. Y. (2005). Friction stir welding and processing. *Mat. Sci. Eng. R*, 50, 1-2, 1-78, 0927-796X

- Morgeneyer, T. F.; Starink, M. J. & Sinclair, I. (2006). Experimental analysis of toughness in 6156 Al-alloy sheets for aerospace applications. *Materials Science Forum*, 519-521, Part 2, 1023-1028, 0255-5476
- Murr, L. E.; Liu, G. & McClure, J. C. (1998). TEM study of precipitation and related microstructures in friction-stir-welded 6061 aluminum. *J. Mat. Sci.*, 33, 5, 1243-1251, 0022-2461
- Murr, L. E. (2010). A Review of FSW Research on Dissimilar Metal and Alloy Systems. *J. Mater. Eng. Perform.*, in press, DOI: 10.1007/s11665-010-9598-0
- Nandan, R.; DebRoy, T. & Bhadeshia, H. K. D. H. (2008). Recent advances in friction-stir welding – Process, weldment structure and properties. *Progress Mater. Sci.*, 53, 6, 980-1023, 0079-6425
- Norman, A. F.; Hyde, K.; Costello, F.; Thompson, S.; Birley, S. & Prangnell, P. B. (2003). Examination of the effect of Sc on 2000 and 7000 series aluminium alloy castings: For improvements in fusion welding. *Mater. Sci. Eng. A*, 354, 1-2, 188-198, 0921-5093
- Papazian, J. M. (1982). Calorimetric studies of precipitation and dissolution kinetics in aluminium alloys 2219 and 7075. *Metall. Trans. A*, 13, 5, 761-769
- Peel, M.; Steuwer, A.; Preuss, M. & Withers, P. J. (2003). Microstructure, mechanical properties and residual stresses as a function of welding speed in aluminium AA5083 friction stir welds. *Acta Mater.*, 51, 16, 4791-4801, 1359-6454
- Priya, R.; Subramanya Sarma, V. & Prasad Rao, K. (2009). Effect of post weld heat treatment on the microstructure and tensile properties of dissimilar friction stir welded AA 2219 and AA 6061 alloys. *Trans. Indian Inst. Metals*, 62, 1, 11-19, 0019-493X
- Reynolds, A. P. (2000). Visualisation of material flow in autogenous friction stir welds. *Sci. Technol. Weld. Join.*, 5, 2, 120-124, 1362-1718
- Reynolds, A. P. (2008). Flow visualization and simulation in FSW. *Scripta Mater.*, 58, 5, 338-342, 1359-6462
- Sato, Y. S.; Kokawa, H.; Enomoto, M. & Jogan, S. (1999). Microstructural evolution of 6063 aluminum during friction-stir welding. *Metall. Mater. Trans. A*, 30, 9, 2429-2439, 1073-5623
- Sato, Y. S. & Kokawa, H. (2001). Distribution of tensile property and microstructure in friction stir weld of 6063 aluminum. *Metall. Mater. Trans. A*, 32, 12, 3023-3031, 1073-5623
- Sato, Y. S.; Urata, M. & Kokawa, H. (2002). Parameters controlling microstructure and hardness during friction-stir welding of precipitation-hardenable aluminum alloy 6063. *Metall. Mater. Trans. A*, 33, 3, 625-635, 1073-5623
- Sauvage, X.; Dèdè, A.; Cabello Muñoz, A. & Huneau B. (2008). Precipitate stability and recrystallisation in the weld nuggets of friction stir welded Al-Mg-Si and Al-Mg-Sc alloys. *Mater. Sci. Eng. A*, 491, 1-2, 364-371, 0921-5093
- Su, J. Q.; Nelson, T. W. & Sterling, C. J. (2003). A new route to bulk nanocrystalline materials. *J. Mat. Res.*, 18, 8, 1757-1760, 0884-2914
- Sullivan, A. & Robson, J. D. (2008). Microstructural properties of friction stir welded and post-weld heat-treated 7449 aluminium alloy thick plate. *Mater. Sci. Eng. A*, 478, 1-2, 351-360, 0921-5093
- Svensson, L. E.; Karlsson, L.; Larsson, H.; Karlsson, B.; Fazzini, M. & Karlsson, J. (2000). Microstructure and mechanical properties of friction stir welded aluminium alloys

- with special reference to AA 5083 and AA 6082. *Sci. Technol. Weld. Join.*, 5, 5, 285-296, 1362-1718
- Thomas, W. M.; Johnson, K. I. & Wiesner, C. S. (2003). Friction stir welding-recent developments in tool and process technologies. *Adv. Eng. Mater.*, 5, 7, 485-490, 1438-1656
- Uematsu, Y.; Tokaji, K.; Shibata, H.; Tozaki, Y. & Ohmune, T. (2009). Fatigue behaviour of friction stir welds without neither welding flash nor flaw in several aluminium alloys. *Int. J. Fatigue*, 31, 10, 1443-1453, 0142-1123
- Uzun, H.; Dalle Donne, C.; Argagnotto, A.; Ghidini, T. & Gambaro, C. (2005). Friction stir welding of dissimilar Al 6013-T4 To X5CrNi18-10 stainless steel. *Mater. Design*, 26, 1, 41-46, 0261-3069
- Yang, Q.; Mironov, S.; Sato, Y. S. & Okamoto, K. (2010). Material flow during friction stir spot welding. *Mater. Sci. Eng. A*, 527, 16-17, 4389-4398, 0921-5093
- Zhao, H., White, D. R. & DebRoy, T. (1999). Current Issues and Problems in Laser Welding of Automotive Aluminum Alloys. *Int. Mater. Rev.*, 44, 6, 238-266, 0950-6608

IntechOpen



Aluminium Alloys, Theory and Applications

Edited by Prof. Tibor Kvackaj

ISBN 978-953-307-244-9

Hard cover, 400 pages

Publisher InTech

Published online 04, February, 2011

Published in print edition February, 2011

The present book enhances in detail the scope and objective of various developmental activities of the aluminium alloys. A lot of research on aluminium alloys has been performed. Currently, the research efforts are connected to the relatively new methods and processes. We hope that people new to the aluminium alloys investigation will find this book to be of assistance for the industry and university fields enabling them to keep up-to-date with the latest developments in aluminium alloys research.

How to reference

In order to correctly reference this scholarly work, feel free to copy and paste the following:

Claudio Badini, Claudia Milena Vega Bolivar, Andrea Antonini, Sara Biamino, Paolo Fino, Diego Giovanni Manfredi, Elisa Paola Ambrosio, Francesco Acerra, Giuseppe Campanile and Matteo Pavese (2011). A Simple Approach to the Study of the Ageing Behaviour of Laser Beam and Friction Stir Welds between Similar and Dissimilar Alloys, Aluminium Alloys, Theory and Applications, Prof. Tibor Kvackaj (Ed.), ISBN: 978-953-307-244-9, InTech, Available from: <http://www.intechopen.com/books/aluminium-alloys-theory-and-applications/a-simple-approach-to-the-study-of-the-ageing-behaviour-of-laser-beam-and-friction-stir-welds-between>

INTech
open science | open minds

InTech Europe

University Campus STeP Ri
Slavka Krautzeka 83/A
51000 Rijeka, Croatia
Phone: +385 (51) 770 447
Fax: +385 (51) 686 166
www.intechopen.com

InTech China

Unit 405, Office Block, Hotel Equatorial Shanghai
No.65, Yan An Road (West), Shanghai, 200040, China
中国上海市延安西路65号上海国际贵都大饭店办公楼405单元
Phone: +86-21-62489820
Fax: +86-21-62489821

© 2011 The Author(s). Licensee IntechOpen. This chapter is distributed under the terms of the [Creative Commons Attribution-NonCommercial-ShareAlike-3.0 License](https://creativecommons.org/licenses/by-nc-sa/3.0/), which permits use, distribution and reproduction for non-commercial purposes, provided the original is properly cited and derivative works building on this content are distributed under the same license.

IntechOpen

IntechOpen